

# Raman spectroscopy and conductivity measurements on polymer-multiwalled carbon nanotubes composites

Christophe Stéphan and Thien Phap Nguyen

Laboratoire de Physique Cristalline, Institut des Matériaux Jean Rouxel, BP 32229, 44322  
Nantes cedex 3, France

Bernd Lahr and Werner Blau

Department of Physics, Trinity College, Dublin 2, Ireland

Serge Lefrant<sup>a)</sup> and Olivier Chauvet

Laboratoire de Physique Cristalline, Institut des Matériaux Jean Rouxel, BP 32229, 44322  
Nantes cedex 3, France

(Received 5 February 2001; accepted 19 November 2001)

Thin films of poly(methyl methacrylate)–multiwalled nanotubes composites were produced by spin coating using different nanotube concentrations. The materials were characterized by scanning electron microscopy, energy-dispersive x-ray analysis, and Raman spectroscopy to obtain information on the possible interactions between the constituents and to control the homogeneity of the films. Electrical conductivity measurements of the composites, as a function of the nanotube concentration, show a percolation threshold at very low concentration. Also, the  $J$ – $E$  characteristics exhibits a nonlinear behavior at low concentration, becoming linear far above the threshold.

## I. INTRODUCTION

Carbon nanotubes belong to a new form of carbon with unique electrical properties. Depending on chirality and diameter, single-walled nanotubes (SWNTs) are expected to be metallic or semiconducting. Wildoer *et al.*<sup>1</sup> and Odom *et al.*<sup>2</sup> confirmed these predictions by measuring the conductivity of individual nanotubes by using a scanning tunneling microscope. Nanotubes are attractive materials for potential applications as field-emission electron sources,<sup>3–6</sup> field effect transistors,<sup>7</sup> etc. Composites based on polymers and nanotubes appear also promising in electronic devices as recently demonstrated with a poly(phenylene vinylene) conjugated polymer/nanotubes system.<sup>8,9</sup> The conductivity of these composites increases as a function of the nanotube concentration by many orders of magnitude.<sup>9</sup> More recently, single-walled nanotubes were blended with poly(methyl methacrylate), a nonconjugated polymer,<sup>10</sup> with the purpose of obtaining flexible and good conductive films which can be of interest as buffer layers in electronics, acting as impedance adaptors.

In this work, we have extended our studies and investigated composites using multiwalled nanotubes (MWNTs) and poly(methyl methacrylate) as the nonconjugated polymer. First, we studied the homogeneity of

the films by scanning electron microscopy (SEM) and energy-dispersive x-ray spectroscopy (EDX). Second, Raman spectroscopy was used to characterize the composites and to examine the possible interactions between the two constituents. We studied also the electrical properties of the composite films by measurements of their conductivity as a function of the nanotube concentration, as well as the current–voltage characteristics in the whole range  $-100$  to  $100$  V, limited to  $-5$  to  $5$  V at high concentration.

## II. EXPERIMENTAL DETAILS

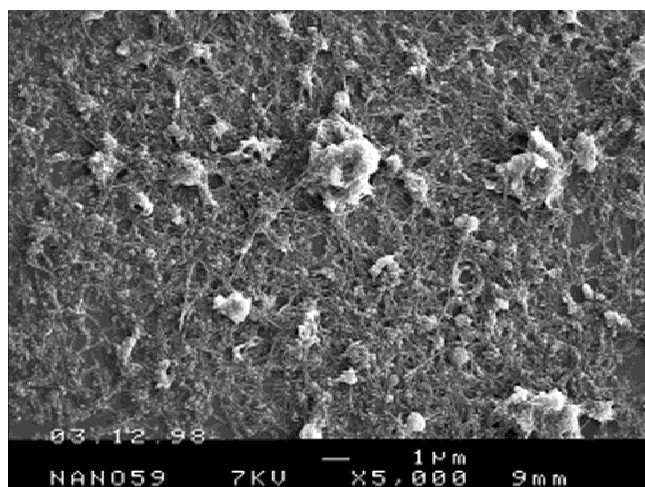
MWNTs produced by the electric arc method<sup>9</sup> and poly(methyl methacrylate) (PMMA) were mixed together in toluene with several concentrations of nanotubes specified by weight percentage in the polymer. The solution was mixed in an ultrasonic bath during 8 h and was immediately deposited by spin coating the solution onto cleaned KBr substrates for Raman spectroscopy and onto glass plates for scanning electron microscopy observations. All Raman measurements were performed at room temperature and in ambient air. The samples used for the current–voltage measurements were obtained also by depositing the solution prepared as described above onto glass substrates covered by bottom chromium electrode. Chromium was also used for the top electrode. Four samples of active area  $2 \times 2$  mm<sup>2</sup> were obtained on the same substrate. The thickness of the films was

<sup>a)</sup>Address all correspondence to this author.  
e-mail: serge.lefrant@cnsr-immn.fr

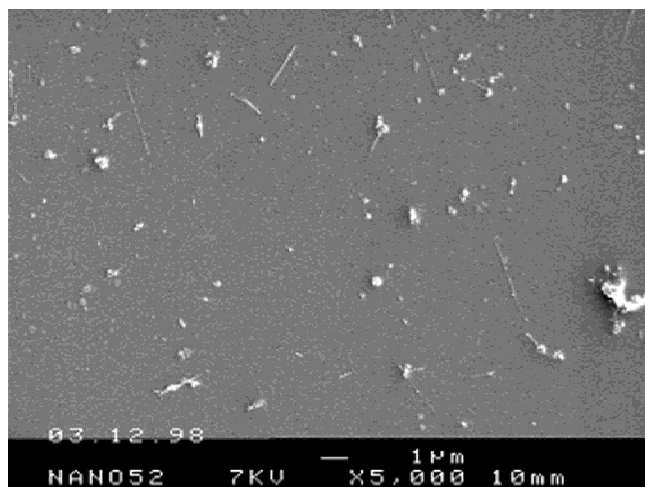
determined by an Alphastep unit and varied from 2 to 4  $\mu\text{m}$ . SEM images of the PMMA–MWNTs composite films were obtained by using a JEOL JSM 6400F microscope (Tokyo, Japan) while EDX analyses were performed on JEOL 5800. The experimental setup used for Raman measurements was an FT Raman Bruker RFS 100 spectrometer (Wisssembourg, France) using an excitation wavelength of 1064 nm. Electrical measurements were performed in vacuum.

### III. SAMPLE CHARACTERIZATION

Figures 1(a) and 1(b) show SEM images of PMMA–MWNTs composites for the 16 and 1 wt% concentrations respectively. In the 16% concentration sample, we observe aggregates emerging from the PMMA matrix. In general, very few aggregates are present in the high-concentration samples. For the 1% concentration, there are apparently no aggregates but only small fibers on the



(a)



(b)

FIG. 1. Scanning electron micrographs (SEM) of the composites films for (a) 16% concentration and (b) 1% concentration.

polymer surface, and the film appears uniform. The quality of the films looks better than the PMMA–SWNTs composite ones.<sup>10</sup> The smaller quantity of amorphous carbon in the MWNTs samples may facilitate a better dispersion of nanotubes in the polymer than with SWNTs materials. EDX analysis of the films, by measuring the [C]/[O] ratio on an estimated area of approximately 0.02 mm<sup>2</sup>, gives a constant ratio over the film which shows a uniform distribution of nanotubes in the polymer at low concentrations (up to 8%). For higher concentrations, the analysis shows a few regions where the quantity of carbon is higher, presumably corresponding to aggregates of nanotubes, as a signature of the presence of almost pure carbon phases.

As already shown in a previous paper,<sup>10</sup> Raman spectroscopy of PMMA–SWNTs composites reveals noticeable modifications in the vibrational bands of nanotubes. It was shown in particular that amorphous carbon was less present in the samples by incorporation in PMMA. Also, it was suggested by the use of simple calculations that the PMMA polymer induces a local pressure on the bundles, as evidence by frequency changes on the low-frequency radial breathing modes.<sup>11</sup> We have carried out the same type of experiments on PMMA–MWNTs composite films. In Fig. 2, we present Raman spectra of such composites at different nanotube concentrations (1, 2, 4, 6, and 8%), recorded with an excitation wavelength of 1064 nm. Here too, we only observe the Raman vibrational modes of MWNTs, resonantly enhanced compared to those of PMMA. It must be noticed that one has to keep the laser power sufficiently low to avoid thermal damage of the composites, since they burn easily whereas PMMA does not under similar conditions. The burning effect is increasing with MWNTs concentration.

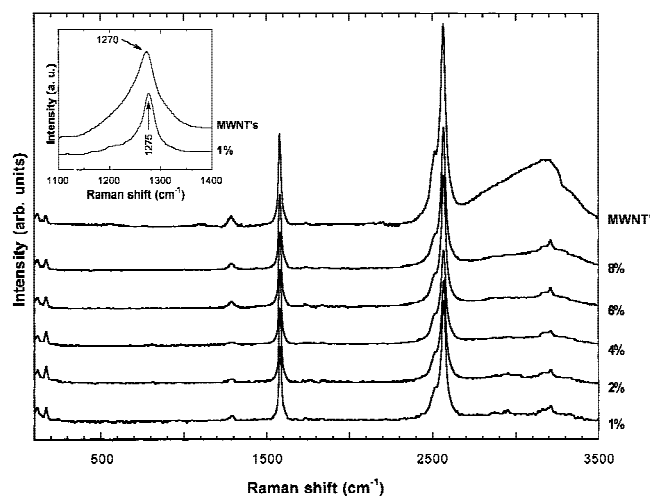


FIG. 2. Raman spectra of MWNTs and PMMA–MWNTs composites for several concentrations (1, 2, 4, 6, and 8%) with 1064-nm excitation. The inset shows details of the “D band” for a 1% PMMA–MWNTs composite and MWNTs.

#### IV. RAMAN SPECTRA

Raman spectra of MWNTs exhibit several features. The so-called graphite mode or “G” band is peaked at  $1581\text{ cm}^{-1}$ . We also observe a rather strong band at  $1270\text{ cm}^{-1}$ , generally seen in carbon nanotubes, attributed to disordered graphitic structures and labeled as the “D” band. As a matter of fact, during the nanotube synthesis, disordered carbonaceous compounds, including amorphous carbon, are produced. We have also shown that intrinsic defects in SWNTs could give a contribution to the Raman scattering in this range of frequency.<sup>12</sup> In the case of MWNTs alone, an asymmetric profile in the low-frequency side of this band is observed, as a possibility of having two distinct contributions. In PMMA–MWNTs composites, this feature is slightly upshifted to  $1275\text{ cm}^{-1}$ , and it is more symmetric, narrower, and less intense compared to the “G” mode. To explain this effect, one can invoke the lower concentration of disordered or amorphous carbon left in the composite during the dispersion step of MWNTs at low concentration. By the way, the “G” band at  $1581\text{ cm}^{-1}$  does not change when MWNTs are introduced in PMMA.

Other important features in the Raman spectra of MWNTs and PMMA–MWNTs composites are observed in the low-frequency range as shown in Fig. 3. They consist of Raman bands peaked at 120, 146, and  $171\text{ cm}^{-1}$ . It is well-known that low-frequency Raman bands appear in SWNTs. They are due to radial breathing modes (RBM) whose frequency is strongly dependent on the diameter. These features have been extensively used

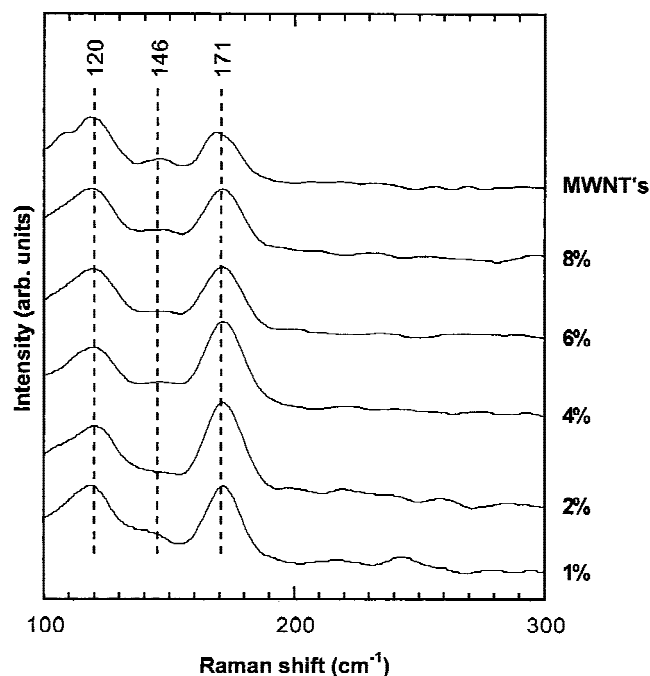


FIG. 3. Details of the low-frequency range Raman spectra of MWNTs and PMMA–MWNTs composites, under the conditions of Fig. 2.

to probe the diameter distributions in SWNTs samples produced by different techniques<sup>13</sup> or to follow synthesis parameters such as temperature, nature, and pressure of inert gas, etc., when changed. We argue here that these low-frequency bands are intrinsic to MWNTs. First, the G band, observed at  $1581\text{ cm}^{-1}$ , exhibits only one component unlike that observed in SWNTs where several other bands are identified. Therefore, taking into account the synthesis conditions (without catalyst), as well as the higher frequency Raman features (shape of G band), one can exclude the presence of SWNTs in our samples. This is corroborated by high-resolution TEM observations. Then, low-frequency Raman modes have already been observed<sup>14–16</sup> in MWNTs samples in particular in purified samples, although their origin has not been clearly identified. Recent calculations performed in our laboratory revealed that the van der Waals interactions between concentric tubes of different diameters could lead to low-frequency breathing modes, the effect of the interactions being to upshift the Raman modes compared to those of individual tubes.<sup>11</sup> Therefore, it is not surprising to observe Raman modes in this range due to MWNTs and definitely not to SWNTs. Further work is under progress to clarify these low-frequency bands in MWNTs samples.

#### V. ELECTRICAL MEASUREMENTS

The current–voltage characteristics of the composites were measured for several nanotube mass ratios in the polymer in the range of 0.25–16%. As shown in Fig. 4, the conductivity increases by introduction of nanotubes in the polymer. The conductivity of pristine PMMA is below  $5 \times 10^{-11}\text{ S/m}$ , at the limit of our measurement

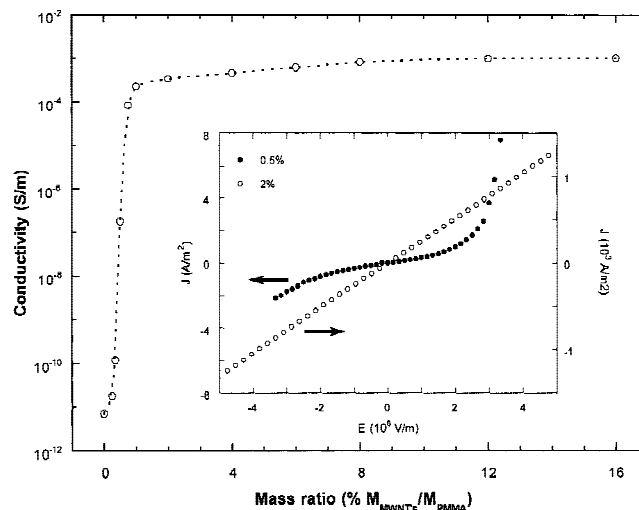


FIG. 4. Plot of the composite conductivity for different nanotube concentrations in PMMA. The dotted line is just a guide for the eye. The current–voltage characteristics of 0.5 and 2% samples are shown in the inset.

capability. Between 0.25 to 1%, we observe a drastic increase to  $2.3 \times 10^{-4}$  S/m. For higher concentrations, the conductivity increases slowly, to reach for the highest concentration sample  $10^{-3}$  S/m. The MWNTs conductivity<sup>17</sup> is approximately  $10^5$  S/m and is much larger than that found in the composites used in these experiments.

This sharp increase of the conductivity is typical of a percolation behavior with a low percolation threshold about 0.5% in mass fraction. For a composite consisting of spherical particles embedded in an insulating matrix, the percolation threshold is expected to be around 33% in volume fraction.<sup>18</sup> Conductivity measurements on aluminum particles–PMMA composites showed a threshold around 25% in volume fraction.<sup>19</sup> However, many factors such as the shape of the filler particles influence the volume percentage needed for conductivity. The elongated shape of nanotubes explains the very low percolation threshold in this system. A similar behavior has been already observed in the case of conducting polymer–poly(vinyl alcohol) composites<sup>20</sup> for example.

The inset in Fig. 4 shows the current–voltage characteristics for films with MWNTs concentrations of 0.5 and 2%, respectively. An ohmic behavior is observed in the 2% sample, and a nonlinear one, in the 0.5% sample. We observe an evolution of the  $I$ – $V$  characteristic as a function of the nanotube concentration: it tends to be ohmic with high concentration ( $>1\%$ ). In the high-concentration regime, there are many conducting paths across the sample with MWNTs connected to each other. It results in a classical ohmic conduction. At low concentration and close to the percolation threshold, less and less conducting paths exist and the nanotubes are separated by the insulating polymer. Nonlinear  $I$ – $V$  characteristics set in due to the charge transfer process from one tube to another across the polymer.

In these electrical measurements, we have shown, via the conductivity dependence versus concentration of MWNTs in the composite, a typical percolation behavior, i.e., starting from the insulator state of PMMA to end up by a sharp transition to a conducting network with a much smaller variation at high MWNTs concentrations. The rather low percolation threshold at  $\rho_c$  approximately 0.5% in mass is due to the large anisotropy of the nanotubes. One can note that, well above  $\rho_c$ , the conductivity is much smaller than that of pure MWNTs. In such cases, this low value (approximately  $10^{-4}$ – $10^{-3}$  S/m) cannot be explained by the ratio in volume occupied by the MWNTs in the composite which provides a strong limitation factor. Thus, one may expect in addition large contact resistances which could also induce a further limitation of the conductivity. A possible role of the contact resistances in the nonlinear  $I$ – $V$  characteristics is not excluded. This is corroborated by the “rectifying like” behavior of Fig. 4 which suggests that the two electrical contacts are not equivalent and play a role in the

conduction of the device. This asymmetry in the current injection from both contacts is likely to be due to the way they have been prepared. The bottom contact has been obtained by spin coating the composite film on an already existing Cr electrode, while the top contact is made by thermal evaporation of Cr on the top on the composite film.

## VI. CONCLUSION

We have shown that the introduction of nanotubes in PMMA increases its conductivity by 9 orders of magnitude. The conductivity measurements as a function of the nanotube concentration indicate that a low concentration of MWNT's (0.5%) is needed for obtaining the percolation threshold. The  $I$ – $V$  characteristics show a nonlinear behavior for low concentrations and became ohmic in the higher concentration samples. The percolation threshold being very low, a small amount of MWNTs is sufficient to realize conducting polymer layer. This can be of real importance in device applications in which light weight conducting films are included, since, at these low MWNTs concentrations, the mechanical properties of the polymer are retained.

## ACKNOWLEDGMENTS

This work has been fully supported by the European Community through its Training and Mobility of Researcher program under network contract [NAMITECH, ERBFMRX-CT96-0067(DG12-MIHT)] and by the French CNRS program (ULTIMATECH).

## REFERENCES

1. J.W.G. Wildöer, L.C. Venema, A.G. Rinzler, R.E. Smalley, and C. Dekker, *Nature* **391**, 59 (1998).
2. T.W. Odom, J.L. Huang, P. Kim, and C.M. Lieber, *Nature* **391**, 62 (1998).
3. W.A. de Heer, A. Châtelain, and D. Ugarde, *Science* **270**, 1179 (1995).
4. O.E. Omel'yanovskii, V.I. Tsebro, O.I. Lebedev, A.N. Kiselev, V.I. Bondareko, N.A. Kiselev, Z. Ja. Kosakovskaja, and L.A. Chernozatonskii, *JETP Lett.* **62**, 503 (1995).
5. Q.H. Wang, T.D. Corrigan, J.Y. Dai, R.P.H. Chang, and A.R. Krauss, *Appl. Phys. Lett.* **70**, 3308 (1997).
6. N.I. Sinityn, Y.V. Gulyaev, G.V. Torgasiov, L.A. Chernozatonskii, Z.Y. Kosakovskaya, Y.F. Zakharchenko, N.A. Kiselev, A.L. Musatov, A.I. Zhanov, S.T. Mevlyut, and O.E. Glukhova, *Appl. Surf. Sci.* **111**, 145 (1997).
7. R. Martel, T. Schmidt, H.R. Shea, T. Hertel, and Ph. Avouris, *Appl. Phys. Lett.* **73**, 2447 (1998).
8. S. Curran, P.M. Ajayan, W.J. Blau, D.L. Carroll, J.N. Coleman, A.B. Dalton, A.P. Davey, A. Drury, B. McCarthy, S. Maier, and A. Stevens, *Adv. Mater.* **10**, 1091 (1998).
9. J.N. Coleman, S. Curran, A.B. Dalton, A.P. Darvey, B. McCarthy, W. Blau, and R.C. Barklie, *Phys. Rev. B* **58**, 7492 (1998).

10. C. Stéphan, T.P. Nguyen, M. Lamy de la Chapelle, S. Lefrant, C. Journet, and P. Bernier, *Synth. Met.* **108**, 139 (2000).
11. J.P. Buisson, O. Chauvet, S. Lefrant, C. Stéphan, and J.M. Benoit, in *Nanotubes and Related Materials*, edited by A.M. Rao, 2000 MRS Fall Meeting, Boston, MA (Warrendale, PA, 2001), p. A14.12.1.
12. M. Lamy de la Chapelle, S. Lefrant, C. Journet, W. Maser, P. Bernier, and A. Loiseau, *Carbon* **36**, 705 (1998).
13. C. Journet, W.K. Maser, P. Bernier, A. Loiseau, M. Lamy de la Chapelle, S. Lefrant, P. Deniard, R. Lee, and J.E. Fischer, *Nature (London)* **388**, 756 (1997).
14. A.V. Bazhenov, V.V. Kveder, A.A. Maksimov, I.I. Tartakovskii, R.A. Oganyan, Y.A. Ossipyan, and A.I. Shalynin, *J. Exp. Theor. Phys.* **86**, 1030 (1998).
15. H. Jantoljak, J.P. Salvetat, L. Forro, and C. Thomsen, *Appl. Phys. A* **67**, 113 (1998).
16. H. Kataura, Y. Achiba, X. Zhao, and Y. Ando, in *Amorphous and Nanostructured Carbon*, edited by J.P. Sullivan, J. Robertston, O. Zhou, J.B. Allen, and B.F. Coll (Warrendale, PA, 2000), p. 113.
17. A.B. Kaiser, G. Düsberg, and S. Roth, *Phys. Rev. B* **57**, 1418 (1998).
18. J. Gurland, *Trans. Met. Soc. AIME* **236**, 642 (1996).
19. V. Singh, A.N. Tiwari, and A.R. Kulkarni, *Mater. Sci. Eng. B* **41**, 310 (1996).
20. M. Makhlouki, M. Morsli, A. Bonnet, A. Conan, A. Pron, and S. Lefrant, *J. Appl. Polym. Sci.* **44**, 443 (1992).